Precise Measurement of Polarization Variation Using Weak Measurement With Double Pointers

Lan Luo [iD], Yu He, Junfan Zhu, Liang Fang [iD], Bo Liu [iD], and Zhiyou Zhang [iD]

Abstract—In this paper, a weak measurement scheme with double pointers (mean value shift and intensity shift of the post-selected light) is presented to simultaneously measure the tiny polarization change (phase and amplitude) of light in a single experimental apparatus. Furthermore, rather than using charge-coupled-device (CCD) to measure the pointer shift, we use the two-channel photoreceiver combined with lock-in amplifier (LIA) to measure the intensities of a split-Gaussian mode in this work. In this way, we introduce two intensity contrast ratios (ICRs) as special pointers to characterize the mean value and intensity shifts. As a result, the measurement precision of the polarization rotation is on the order of magnitude of $10^{-7} rad$ in the experiment. These findings provide a distinctive insight into the weak measurement and have important implications for the accurate measurement of complex optical parameters.

Index Terms—Phase and amplitude, precise measurement, weak measurement.

I. INTRODUCTION

IN OPTICAL measurement, the estimation of the polarization state of light (including the phase and amplitude) provides the essential information about objects. Simultaneously estimating the relative variations of the phase and amplitude of two basis vectors has potential applications in many fields, including the detection of optical rotatory dispersion (ORD) and circular dichroism (CD), the measurement of complex optical susceptibility of materials, and the observation of magneto-optic Faraday and Kerr effects. [1], [2], [3], [4], [5] In general, the

phase and amplitude variations carrying the information on the medium through which the light passed at the same time, resulting in the changes of intensity contrast or polarization rotation. Ellipsometry is the most widely used phase and amplitude measurement technique. In the past century, researchers were working hard to improve the performance of ellipsometry and have developed several new ellipsometers for practical applications, including rotary polarization ellipsometers, phase-modulated ellipsometers, spectroscopic ellipsometry, generalized ellipsometer, etc [6], [7], [8], [9], [10], [11], [12], [13]. The stability of the system, the nonlinear effect of the detector, the instability of the light source, and the azimuth deviation will limit the improvement of the measuring precision of the ellipsometer. In addition, traditional phase and amplitude measurement methods also include Kramers-Kronig relations [14], [15], and Fourier transform spectral interferometry [2], [16], among others. Nevertheless, these methods are affected by instrument and environmental noise, and cannot meet the requirements of higher precision measurement. How to further improve the measurement precision of the polarization change of light, so as to realize the detection of tiny changes in target has always been a concern.

Weak measurement, proposed by Aharonov et al. [17], is a precise method to determine the statistical properties of quantum systems by using pre- and post-selections under the condition of weak coupling between the system and the meter. Based on weak value amplification, weak measurement has been widely used in the measurement of various tiny parameters [18], [19], [20], [21], [22], [23], [24] The real and imaginary parts of complex weak values correspond to these different effects [25], [26], [27], [28]. For the measurement of the quantum wave function of the particle, the real and imaginary parts of the weak value are proportional to the real and imaginary parts of the wave function [29], [30]. By using a pointer state endowed with orbital angular momentum (OAM), the real and imaginary parts of the weak-value of a polarization operator are respectively related to the expected value of the two conjugate variables of the pointer [31], [32], [33], [34]. The complex nature of the weak value could also be used to measure the complex optical parameters [35], [36], [37]. However, these methods have some indirection in measuring the changes in polarization of the light since the real and imaginary parts of the signal are estimated separately.

In this paper, we propose a weak measurement method with double pointers (mean value and intensity shift) to estimate the phase and amplitude variations simultaneously. The probability

Lan Luo is with the Key Laboratory of Science and Technology on Space Optoelectronic Precision Measurement, CAS, Chengdu 610209, China, and also with the Institute of Optics and Electronics, Chinese Academy of Sciences, Chengdu 610209, China (e-mail: naloul@163.com).

Yu He was with the College of Physics, Sichuan University, Chengdu 610064, China. She is now with the College of Optoelectronic Engineering, Chengdu University of Information Technology, Chengdu, Sichuan 610225, China (e-mail: heyu@cuit.edu.cn).

Junfan Zhu and Zhiyou Zhang are with the College of Physics, Sichuan University, Chengdu 610064, China (e-mail: 893608884@qq.com; zhangzhiyou@scu.edu.cn).

Liang Fang and Bo Liu are with the Key Laboratory of Science and Technology on Space Optoelectronic Precision Measurement, CAS, Chengdu 610209, China, also with the Institute of Optics and Electronics, Chinese Academy of Sciences, Chengdu 610209, China, and also with the University of Chinese Academy of Sciences, Beijing 100049, China (e-mail: fangl@ioe.ac.cn; boliu@ioe.ac.cn).

This article has supplementary downloadable material available at https://doi.org/10.1109/JPHOT.2023.3281586, provided by the authors.

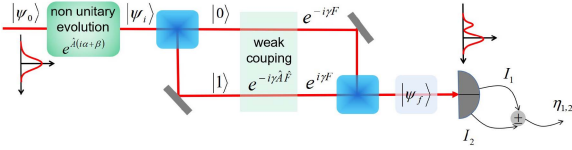Digital Object Identifier 10.1109/JPHOT.2023.3281586

Fig. 1. Schematic diagram of double pointers weak measurement scheme using two-channel detection. The non-unitary evolution corresponds to the phase and amplitude changes of light, that is, the parameters to be measured.

distribution of the post-selected light follows a bimodal function when the initial meter is Gaussian. Therefore, we propose to use a two-channel photoreceiver combined with a lock-in amplifier (LIA) to measure split-Gaussian and introduce the double intensity contrast ratios (ICRs) to characterize the double pointers. It demonstrates that the ICR η_1 is positively correlated with the phase, while the ICR η_2 is related to both the phase and amplitude variations. Therefore, using the two-channel measurement method, the phase and amplitude changes can be measured simultaneously in a single experimental apparatus. Experimental results demonstrate the high precision and feasibility of this method.

II. THEORETICAL ANALYSIS

The experimental scheme for the polarization measurement based on weak measurement is shown in Fig. 1. Firstly, consider a joint state expressed as $|\psi_0\rangle \otimes |\phi\rangle$, where $|\psi_0\rangle = (|0\rangle + |1\rangle)/\sqrt{2}$ is the incident polarization state of the light, and $|\phi\rangle = \int dF |F\rangle|\phi(F)$ denotes the meter's distribution function. $\phi(F) = 1/(\pi\Delta F^2)^{1/4} \exp(-F^2/2\Delta F^2)$. Here, $|0\rangle$ and $|1\rangle$ represent the eigenstates of the observable operator $\hat{A} = |0\rangle\langle 0| - |1\rangle\langle 1|$. $\hat{F}$ is the input variable for the instrument, and ΔF represents the uncertainties of $\hat{F}$.

Assume that the incident light is prepared under the polarization state given in the following formula

$$|\psi_i\rangle = \exp(i\alpha)\cos\left(\frac{\pi}{4}+\beta\right)|0\rangle + \exp(-i\alpha)\sin\left(\frac{\pi}{4}+\beta\right)|1\rangle$$

$$\approx \frac{1}{\sqrt{2}}\left[\exp\left(i\alpha+\beta\right)|0\rangle + \exp\left(-i\alpha-\beta\right)|1\rangle\right]$$

$$= \exp[(i\alpha+\beta)\hat{A}]|\psi_0\rangle, \tag{1}$$

here, $\alpha << 1$ and $\beta << 1$ represent the tiny phase and amplitude changes between the $|0\rangle$ and $|1\rangle$, which are related to the polarization rotation and ellipticity of the elliptical polarization. In the weak measurement model, the interaction between the system and the meter is expressed by a unitary operator $\hat{U} = \exp(-i\gamma\hat{A} \otimes \hat{F})$, where $\gamma << 1$ represents the coupling strength of the interaction. After being projected onto the following post-selected states

$$|\psi_f\rangle = (|0\rangle - |1\rangle)/\sqrt{2}, \tag{2}$$

the whole state evolves into

$$|\Psi\rangle = \int dF |F\rangle|\phi(F)\rangle\left\langle\psi_f\left|\exp\left(-i\gamma\hat{A}\otimes\hat{F}\right)\right|\psi_i\right\rangle$$

$$= \int dF |F\rangle|\phi(F)\langle\psi_f|\psi_i\rangle\left[\cos(\gamma F) - iA_\omega\sin(\gamma F)\right], \tag{3}$$

where $A_\omega = \langle\psi_f|\hat{A}|\psi_i\rangle/\langle\psi_f|\psi_i\rangle$ denotes the weak value of $\hat{A}$, and $|\langle\psi_f|\psi_i\rangle|^2 = (\cosh 2\beta - \cos 2\alpha)/2$ is the post-selection probability. Here, the imaginary and real parts of the weak-value, respectively, take the forms

$$\Im(A_w) = \frac{\sin 2\alpha \cos 2\beta}{\cos 2\alpha \cos 2\beta - 1}, \tag{4}$$

$$\Re(A_w) = \frac{\sin 2\beta}{\cos 2\alpha \cos 2\beta - 1}. \tag{5}$$

The light field distribution is $\langle\Psi|\Psi\rangle = \int dF[-\cos(2\alpha - 2\gamma F) + \cosh 2\beta]\phi(F)^2/2$. And the intensity of the post-selected light is expressed as

$$I_t = I_0 \langle\Psi|\Psi\rangle$$

$$= \frac{I_0}{2}|\langle\psi_f|\psi_i\rangle|^2\left[\left(1-|A_w|^2\right)e^{-\Delta F^2\gamma^2} + 1 + |A_w|^2\right]$$

$$= \frac{I_0}{4}\left[1 - \exp\left(-\Delta F^2\gamma^2\right)\cos 2\alpha \cos 2\beta\right]. \tag{6}$$

here, I_0 is the initial intensity of the light without post-selection. The pointer of the mean value can be obtained as

$$\delta F = \frac{\langle\Psi|\hat{F}|\Psi\rangle}{\langle\Psi|\Psi\rangle}$$

$$= \frac{2\Im(A_w)\gamma\Delta F^2}{1-|A_w|^2 + (1+|A_w|^2)e^{\Delta F^2\gamma^2}}$$

$$= \frac{\gamma\Delta F^2 \sin 2\alpha \sin 2\beta}{\cos 2\alpha \cos 2\beta - \exp(\Delta F^2\gamma^2)}. \tag{7}$$

Another pointer is the shift of the total post-selected intensity, which expressed as

$$\eta = \frac{I_t|_{\alpha,\beta} - I_t|_{\alpha=0,\beta=0}}{I_t|_{\alpha=0,\beta=0}} \approx 2\frac{\alpha^2 + \beta^2}{\Delta F^2\gamma^2} \tag{8}$$

It is worth noting that the product of the post-selected light intensity and mean values shows results related only to phase $I_t\delta F = \langle\Psi|\hat{F}|\Psi\rangle \approx -I_0\gamma\Delta F^2 \sin 2\alpha/2$, which also could be considered as the mean value without normalization. To make the calculation easier, we modify the mean value shift

$$\delta F' = \frac{I_t|_{\alpha,\beta}}{I_t|_{\alpha=0,\beta=0}}\delta F \approx -\frac{\sin 2\alpha}{\gamma}. \tag{9}$$

Therefore, we could obtain the phase and amplitude variations in a simpler manner according to (8) and (9). Using the double pointers, only one charge-coupled-device (CCD) can measure the mean value and light intensity at the same time, so as to obtain the changes in the phase and amplitude simultaneously.

In general, the pointer of the standard weak measurement is the shift of mean value of a Gaussian mode [38], such as momentum, coordinate, time and frequency. However, the mean value pointer needs a detector with high resolution and a wide measurement range. In addition, when weak measurement is applied to a quantum light source and a single photon counter,

the detector cannot directly measure the light field distribution to obtain the pointer of mean value with high precision. Therefore, it is of great value and significance to expand the weak measurement pointer system and verify its application.

In this work, we propose using the two-channel photoreceiver combined with the LIA or single-photon counter to characterize the output results. When the initial meter is Gaussian, which is a common meter distribution for weak measurement schemes, the probability distribution of the post-selected light follows a bimodal function. The left and right sides of the post-selected light distribution were received by the two-channel measurement scheme. In Ref. [20], [23], the split-detector is used to measure the average position. In this work, according to the light intensity output by the two-channel detector, two intensity contrast ratios (ICRs) are introduced as special pointers

$$
\begin{aligned}
\eta_1 &= \frac{I_1|_{\alpha,\beta} - I_2|_{\alpha,\beta}}{I_1|_{\alpha=0,\beta=0} + I_2|_{\alpha=0,\beta=0}} \\
&\approx -\frac{2\sin 2\alpha}{\gamma \Delta F \sqrt{\pi}} \propto \delta F', \quad (10)
\end{aligned}
$$

$$
\begin{aligned}
\eta_2 &= \frac{(I_1|_{\alpha,\beta} + I_2|_{\alpha,\beta}) - (I_1|_{\alpha=0,\beta=0} + I_2|_{\alpha=0,\beta=0})}{I_1|_{\alpha=0,\beta=0} + I_2|_{\alpha=0,\beta=0}} \\
&\approx \frac{1 - \cos 2\alpha \cos 2\beta}{\Delta F^2 \gamma^2} \\
&\approx 2\frac{\alpha^2 + \beta^2}{\Delta F^2 \gamma^2} = \eta, \quad (11)
\end{aligned}
$$

where $I_1|_{\alpha,\beta} = \int_0^\infty \langle \Psi | \Psi \rangle \, dF$ and $I_2|_{\alpha,\beta} = \int_{-\infty}^0 \langle \Psi | \Psi \rangle \, dF$ represent the intensities of the left- and right- sides of the post-selected light distribution, which can be simultaneously received by the two-channel detector. According to (10) and (11), the dynamic measurement range of the phase is $-\pi/4 < \alpha < \pi/4$, while the amplitude is $-\pi/2 < \beta < 0$ or $0 < \beta < \pi/2$. However, as the phase and amplitude shifts increase, the light intensity variation is much lower than the total light intensity, making it impossible for the detector to obtain the light intensity changes. Therefore, although this scheme provides a very large dynamic range, it is only suitable for measuring tiny phase and amplitude changes while considering measurement precision.

It is worth noting that η_1 is positively related to the modified mean shift $\delta F'$, whereas η_2 is the intensity shift pointer η. As a result, using (10) and (11), we can obtain the phase and amplitude variations with two-channel detection. Compared with direct measurement of CCD, two-channel photoreceiver can be connected with a single photon counter or phase-locked amplifier to further improve measurement precision.

According to (10) and (11), the ICRs (η_1 and η_2) as functions of the polarization variation (phase and amplitude) without any approximation are shown in Fig. 2(a) and (b). It is worthwhile to note that η_1 is proportional to the phase change and is completely unaffected by the amplitude change. η_2 is related to both phase and amplitude variations. However, η_2 does not change linearly with the amplitude, and the measurement sensitivity is very small when the amplitude variation tends to 0. Those issues can be
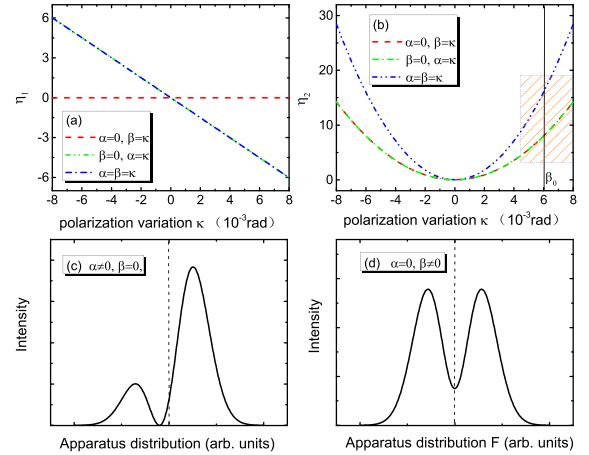

Fig. 2. (a) and (b) show the changes of two intensity ratios (η_1 and η_2) under different different phase and amplitude shifts. (c) and (d) show the light field distribution in the case of $\beta = 0$ and $\alpha = 0$, respectively. Here, $\Delta F = 10^2$ and $\gamma = 10^{-5}$.

resolved by introducing the modulation weak measurement technique [39], [40]. An appropriate modulated amplitude parameter β_0 is introduced, and we perform the following transformation

$$
\beta \rightarrow \beta' = \beta_0 + \beta. \quad (12)
$$

By this way, the measurement area falls into the measurement shadow area in Fig. 1(b), and the polarization rotation estimation can be carried out in the linear dynamic measurement area with high sensitivity.

According to the above theoretical analysis, we can know that the influence of phase and amplitude changes on the meter distribution is completely different. In order to further explain the effect of phase and amplitude variations on the light field, the distributions of the post-selected light fields with different phase and amplitude variations are shown in Fig. 2(c) and (d). The existence of phase change will produce an asymmetric split-Gaussian beam, see Fig. 2(c). In the case of only amplitude change, the light field is a symmetric split-Gaussian, see Fig. 2(d). The light field distribution variation trend is consistent with the results of (10) and (11).

III. EXPERIMENTAL SETUP AND RESULTS

An experiment is performed to prove the validity of the present weak measurement method. The experiment setup is shown in Fig. 3, where we consider the left- and right-circular polarization ($|+\rangle$ and $|-\rangle$) as an example of the eigenvectors ($|0\rangle$ and $|1\rangle$). Firstly, the light beam is generated by a He-Ne laser (Thorlabs HNL210) at the wavelength of 632.8 nm. The acousto–optic modulator (AOM) is controlled by the Function generator and generates a Transistor-Transistor Logic (TTL) with a duty cycle of 1:1 at a frequency of 25 kHz. The light beam is then passed through a half wave plate (HWP), a short focal length lens (L1, f = 50 mm, corresponding to the beam waist $w = 27$um), and the first Glan polarizer (P1). The combination of the HWP and P1 can be used to adjust the incident light intensity to avoid the saturation of the detector. The optical axis of the P1 is placed in
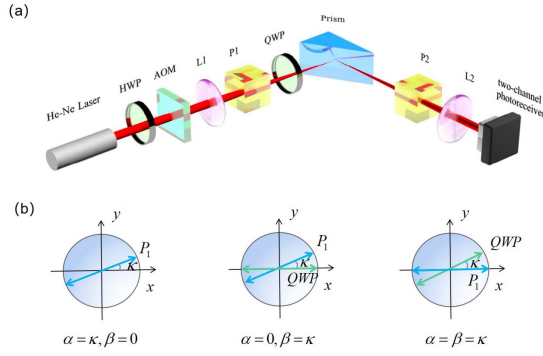
Fig. 3. The experimental setup for estimating the phase and amplitude shifts simultaneously. Light source, He-Ne laser; HWP, half-wave plate; AOM, acousto–optic modulator, L1 and L2, lenses of focal length 50 mm and 250 mm, respectively; P1 and P2, Glan laser polarizers; QWP, binary compound zero-order quarter wave plate. (b) Three different polarization variations are to be estimated.

the horizontal direction to prepare the incident polarization state

$$|\psi_0\rangle = (|+\rangle + |-\rangle)/\sqrt{2} = |H\rangle, \tag{13}$$

where $|\pm\rangle = (|H\rangle \pm i|V\rangle)/\sqrt{2}$. $|H\rangle$ and $|V\rangle$ are the horizontal and vertical polarization states. The combination of a quarter wave plate (QWP) and the P1 is used to prepare different pre-selections

$$|\psi_i\rangle = \frac{1}{\sqrt{2}} \left[\exp(i\alpha - \beta)|-\rangle + \exp(-i\alpha + \beta)|+\rangle \right]$$
$$\approx |H\rangle + |V\rangle(\alpha + i\beta). \tag{14}$$

Here, $\alpha \ll 1$ and $\beta \ll 1$ represent the tiny phase and amplitude changes between the $|+\rangle$ and $|-\rangle$. As shown in Fig. 3(b), in the case without the QWP, by rotating the optical axis of P1 with respect to the vertical direction, the porization state $|H\rangle + \alpha|V\rangle$ is obtained. In the case of existence of the QWP, the light state $|H\rangle + i\beta|V\rangle$ is produced by rotating P1, and $|H\rangle + (\alpha + i\beta)|V\rangle$ is produced by rotating QWP ($\alpha = \beta$). The input pointer state is $|\phi_m\rangle = \int dk_y \varphi(k_y)|k_y\rangle$, where k_y represents the transverse wave-vector component. $\varphi(k_y) = (w/\sqrt{2\pi}) \exp(-w^2 k_y^2/4)$ is the transverse distribution of the pointer wave function.

The light is reflected at the surface of a BK7 prism ($n = 1.515$), the Spin Hall effect of light (SHEL) takes place. According to the relationship between reflected angular spectrum and boundary distribution of the electric field, the polarization state of the light evolves into

$$|\Psi_i\rangle = \hat{U}\hat{R}|\psi_i\rangle \otimes |\phi_m\rangle, \tag{15}$$

where

$$\hat{U} = \exp(-ik_y\delta\hat{\sigma}_3) \tag{16}$$

represents the unitary evolution to describe the spin splitting of the SHEL and

$$\hat{R} = \frac{1}{2}\begin{bmatrix} r_p + r_s & r_p - r_s \\ r_p - r_s & r_p + r_s \end{bmatrix} \tag{17}$$

describes the changes in horizontal and vertical polarization due to reflection. $\hat{\sigma}_3 = |+\rangle\langle+| - |-\rangle\langle-|$ represents the spin

operator of a photon. δ is the original spin splitting induced by SHEL, which plays the roles of the weak coupling between the system and the meter. r_p and r_s denote the Fresnel reflection coefficients of the horizontal and vertical polarization, respectively. In the experiment, the incident angle is set as $\theta = 40°$. Therefore, the corresponding reflection coefficients are $r_p = 0.123$ and $r_s = -0.28$. The original shift $\delta \approx 0.15\,\mathrm{um}$. In addition, $|\psi_m\rangle = \hat{R}|\psi_i\rangle$ is regarded as the pre-selection in the weak measurement model.

Next, the axis of the second Glan polarizer (P2) is placed in the vertical direction to produce the post-selection

$$|\psi_f\rangle = (|+\rangle - |-\rangle)/\sqrt{2} = |V\rangle. \tag{18}$$

Therefore, the whole system can be expressed as

$$|\Psi_f\rangle = \langle\psi_f|\exp(-ik_y\delta\hat{\sigma}_3)|\psi_m\rangle|\phi_m\rangle. \tag{19}$$

Finally, after being collimated by the second lens (L2), the light is recorded by the two-channel photoreceiver (Hamamatsu, S4204), in which the upper and lower parts of the light field enter the two ports of the detector respectively. The two-channel photoreceiver is connected to a low-noise amplification circuit (NF, CA5350) and a LIA (Stanford Research System, SR865 A) to output the light intensities. Since the signal read in this experiment is a static output value, the lock-in time constant is set as 1 sec. to suppress the fluctuation of the input. Compared with CCD, this detection terminal can better suppress the electronic noise, environmental noise, and light intensity instability of the light on the measurement and further improve the measurement precision. Therefore, two ICRs are respectively expressed as

$$\eta_1 = \frac{I_1|_{\alpha,\beta} - I_2|_{\alpha,\beta}}{I_t|_{\alpha=0,\beta=0}} \approx -\sqrt{\frac{2}{\pi}}\frac{r_s w}{r_p \delta}\sin 2\alpha, \tag{20}$$

$$\eta_2 = \frac{(I_1|_{\alpha,\beta} + I_2|_{\alpha,\beta}) - I_t|_{\alpha=0,\beta=0}}{I_t|_{\alpha=0,\beta=0}}$$
$$\approx \frac{r_s^2 w^2}{r_p^2 \delta^2}(\alpha^2 + \beta^2), \tag{21}$$

where $I_1|_{\alpha,\beta} = I_0 \int_0^\infty \langle\Psi_f | \Psi_f\rangle dk_y$ and $I_2|_{\alpha,\beta} = I_0 \int_{-\infty}^0 \langle\Psi_f | \Psi_f\rangle dk_y$ are the two-channel detector's light intensity outputs. Here, I_0 denotes the intensity of the light without post-selection. In the experiment, the initial intensity is set as $I_0 = 18\,mW$. $I_t|_{\alpha=0,\beta=0} = I_1|_{\alpha=0,\beta=0} + I_2|_{\alpha=0,\beta=0}$ represents the total intensity of the post-selected light without phase or amplitude variation. Without introducing phase and amplitude changes, the distribution of the post-selected light follows a bimodal distribution. At this time, $I_t|_{\alpha=0,\beta=0}$ is obtained, which does not change in the subsequent measurement process.

The experimental results, along with the theoretical predictions without any approximation obtained from (20) and (21), are shown in Fig. 4. For the case without the amplitude change ($\beta = 0$), η_1 and η_2 exhibit high sensitivity to phase variation, see Fig. 4(a) and (b). In the absence of phase variation ($\alpha = 0$), η_2 responds sensitively to amplitude variations while η_1 does not, as shown in Fig. 4(c) and (d). In the presence of phase and amplitude variations ($\alpha = \beta = \kappa$), the experimental results in Fig. 4(e) are similar to those in Fig. 4(a), indicating that the
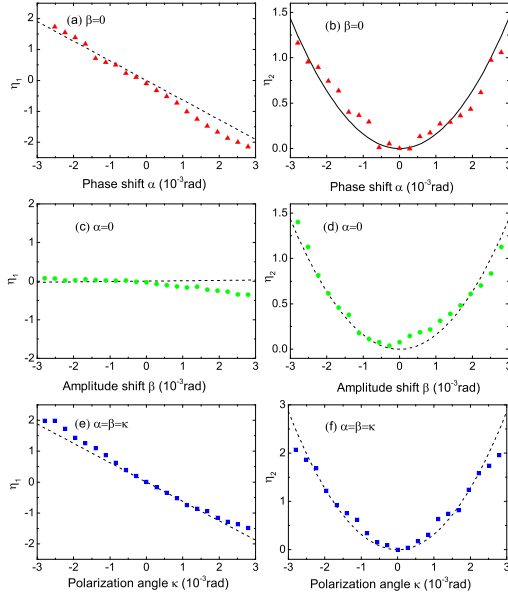
Fig. 4. Experimental and theoretical results for the measurement of different phase and amplitude shifts. The left column represents the ICR η_1 and the right column represents the ICR η_2.
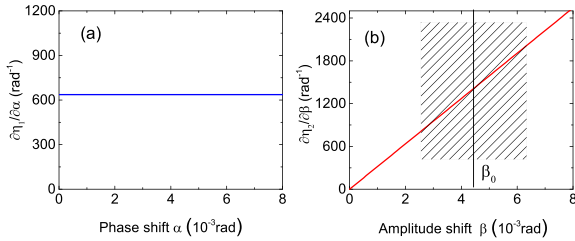

Fig. 5. (a) Shows the sensitivity $\partial\eta_1/\partial\alpha$ changing with phase. (b) Shows the sensitivity $\partial\eta_2/\partial\beta$ to amplitude parameter.

existence of the amplitude variation has no effect on the η_1. After obtaining the phase variation, the amplitude variation can be obtained according to the results of Fig. 4(f). This is also the main advantage of the present method.

The precision of the phase and amplitude variations is obtained by using $\Delta\alpha = \Delta\eta_1/(\partial\eta_1/\partial\alpha)$ and $\Delta\beta = \Delta\eta_2/(\partial\eta_2/\partial\beta)$, respectively. Here $\Delta\eta_1$ and $\Delta\eta_2$ represent the standard deviations of experimentally measured values. In order to estimate the $\Delta\eta_1$ and $\Delta\eta_2$, the post-selected intensity (I_1 and I_2) was recorded 30 times with an interval of 0.2 sec. by the detector, which is limited under 9.2×10^{-5}. In terms of the simulated results of this scheme, Fig. 5(a) shows that the sensitivity of the η_1 to the phase α is a constant with a continuously varying phase, and Fig. 5(b) shows that the sensitivity of the ICR η_2 to the amplitude β tends to increase with β. However, when the amplitude parameter tends to zero, the sensitivity $\partial\eta_2/\partial\beta$ changing with amplitude shift is close to zero. According to the previous analysis, the modulation weak measurement could be introduced to maintain a high measurement sensitivity and linear dynamic range of amplitude measurement by using (12) to make the measurement area fall in the shadow area of Fig. 5(b). As a result, the measurement precision of phase and amplitude is calculated to be $1.4 \times 10^{-7}rad$. Our results far exceed the ellipsometers

($\sim 10^{-4}rad$) [10], [11], and are better than the standard weak measurement scheme using a CCD ($\sim 10^{-5}rad$) [24], [37].

IV. CONCLUSION

To conclude, we have provided a weak measurement scheme with double pointers (mean value and intensity shifts) to estimate tiny polarization variation with high preision. We also propose to use the two-channel photoreceiver combined with a locked-in amplifier (or single-photon counter) to replace the CCD in the conventional weak measurement scheme to measure intensities in split-Gaussian mode. The double ICRs were introduced to characterize mean value shift and intensity shift pointers. It is demonstrate that the ICR η_1 is only affected by the phase varia- tion, while the ICR η_2 is related to both the phase and amplitude changes. Due to the fact that η_1 and η_2 can be measured at the same time, the phase and amplitude variations can be found with a direct measurement. The presented technique no longer requires high-resolution detectors and multiple measurements to obtain phase and amplitude changes. We believe that the present scheme is a low-cost, simple device and easy operation technique, and may have a promising application prospect for estimating complex optical parameters from circular dichroism and optical rotatory dispersion.

REFERENCES

[1] J. Helbing and M. Bonmarin, "Vibrational circular dichroism signal enhancement using self-heterodyning with elliptically polarized laser pulses," *J. Chem. Phys.*, vol. 131, 2009, Art. no. 174507.

[2] H. Rhee et al., "Femtosecond characterization of vibrational optical activ- ity of chiral molecules," *Nature*, vol. 458, pp. 310–313, 2009.

[3] P. Stephens, F. Devlin, J. Cheeseman, M. Frisch, O. Bortolini, and P. Besse, "Determination of absolute configuration using ab initio calculation of optical rotation," *Chi- Rality*, vol. 15, pp. S57–S64, 2003.

[4] F. Yao et al., "Measurement of complex optical susceptibility for individual carbon nanotubes by elliptically polarized light excitation," *Nat. Commun.*, vol. 9, 2018, Art. no. 3387.

[5] R. Shimano et al., "Quantum Faraday and Kerr rotations in graphene," *Nat. Commun.*, vol. 4, 2013, Art. no. 1841.

[6] F. L. McCrackin, E. Passaglia, R. R. Stromberg, and H. L. Steinberg, "Measurement of the thickness and refractive index of very thin films and the optical properties of surfaces by ellipsometry," *J. Res. Nat. Bur. Standards. Sect. A., Phys. Chem.*, vol. 67, 1963, Art. no. 363.

[7] C. V. Kent and J. Lawson, "A photoelectric method for the determination of the parameters of elliptically polarized light," *J. Opt. Soc. Amer.*, vol. 27, pp. 117–119, 1937.

[8] A. Rothen, "The ellipsometer, an apparatus to measure thicknesses of thin surface films," *Rev. Sci. Instrum.*, vol. 16, pp. 26–30, 1945.

[9] K. Vedam, "Spectroscopic ellipsometry: A historical overview," *Thin Solid Films*, vol. 313, pp. 1–9, 1998.

[10] R. Petkovšek, J. Petelin, J. Možina, and F. Bammer, "Fast ellipsometric measurements based on a single crystal photo-elastic modulator," *Opt. Exp.*, vol. 18, pp. 21410–21418, 2010.

[11] D. E. Aspnes and A. A. Studna, "High precision scanning ellipsometer," *Appl. Opt.*, vol. 14, pp. 220–228, 1975.

[12] Y.-T. Kim, R. Collins, and K. Vedam, "Fast scanning spectroelectrochemi- cal ellipsometry: In-situ characterization of gold oxide," *Surf. Sci.*, vol. 233, pp. 341–350, 1990.

[13] G. E. Jellison and F. A. Modine, "Two-modulator generalized ellipsometry: Theory," *Appl. Opt.*, vol. 36, pp. 8190–8198, 1997.

[14] R. d. L. Kronig and H. Kramers, "Zur theorie der absorption und dispersion in den rontgenspektren," *Zeitschrift Fur Physik*, vol. 48, pp. 174–179, 1928.

[15] J. S. Toll, "Causality and the dispersion relation: Logical foundations," *Phys. Rev.*, vol. 104, 1956, Art. no. 1760.

[16] L. Lepetit, G. Cheriaux, and M. Joffre, "Linear techniques of phase measurement by femtosecond spectral interferometry for applications in spectroscopy," *J. Opt. Soc. Am B*, vol. 12, pp. 2467–2474, 1995.

[17] Y. Aharonov, D. Z. Albert, and L. Vaidman, "How the result of a measurement of a component of the spin of a spin-1/2 particle can turn out to be 100," *Phys. Rev. Lett.*, vol. 60, 1988, Art. no. 1351.

[18] O. Hosten and P. Kwiat, "Observation of the spin hall effect of light via weak measurements," *Science*, vol. 319, pp. 787–790, 2008.

[19] Y. Qin, Y. Li, H. He, and Q. Gong, "Measurement of spin hall effect of reflected light," *Opt. Lett.*, vol. 34, pp. 2551–2553, 2009.

[20] P. B. Dixon, D. J. Starling, A. N. Jordan, and J. C. Howell, "Ultrasensitive beam deflection measurement via in-terferometric weak value amplification," *Phys. Rev. Lett.*, vol. 102, 2009, Art. no. 173601.

[21] H. Luo, X. Zhou, W. Shu, S. Wen, and D. Fan, "Enhanced and switchable spin hall effect of light near the Brewster angle on reflection," *Phys. Rev. A*, vol. 84, 2011, Art. no. 043806.

[22] N. Brunner and C. Simon, "Measuring small longitudinal phase shifts: Weak measurements or standard interferometry?," *Phys. Rev. Lett.*, vol. 105, 2010, Art. no. 010405.

[23] D. J. Starling, P. B. Dixon, A. N. Jordan, and J. C. Howell, "Precision frequency measurements with interferometric weak values," *Phys. Rev. A*, vol. 82, 2010, Art. no. 063822.

[24] X. Qiu, L. Xie, X. Liu, L. Luo, Z. Zhang, and J. Du, "Estimation of optical rotation of chiral molecules with weak measurements," *Opt. Lett.*, vol. 41, pp. 4032–4035, 2016.

[25] Y. Aharonov and L. Vaidman, "Properties of a quantum system during the time interval between two measurements," *Phys. Rev. A*, vol. 41, pp. 11–20, 1990.

[26] J. Lundeen and K. Resch, "Practical measurement of joint weak values and their connection to the annihilation operator," *Phys. Rev. A*, vol. 334, pp. 337–344, 2005.

[27] R. Jozsa, "Complex weak values in quantum measurement," *Phys. Rev. A*, vol. 76, 2007, Art. no. 044103.

[28] A. G. Kofman, S. Ashhab, and F. Nori, "Nonperturbative theory of weak pre- and post-selected measurements," *Phys. Rep.*, vol. 520, pp. 43–133, 2012.

[29] J. S. Lundeen, B. Sutherland, A. Patel, C. Stewart, and C. Bamber, "Direct measurement of the quantum wave-function," *Nature*, vol. 474, pp. 188–191, 2011.

[30] C.-R. Zhang et al., "Direct measurement of the two-dimensional spatial quantum wave function via strong measurements," *Phys. Rev. A*, vol. 101, 2020, Art. no. 012119.

[31] O. S. Magana Loaiza, M. Mirhosseini, B. Rodenburg, and R. W. Boyd, "Amplification of angular rotations using weak measurements," *Phys. Rev. Lett.*, vol. 112, 2014, Art. no. 200401.

[32] M. Mirhosseini, O. S. Magana Loaiza, C. Chen, S. M. Hashemi Rafsanjani, and R. W. Boyd, "Wigner distribution of twisted photons," *Phys. Rev. Lett.*, vol. 116, 2016, Art. no. 130402.

[33] H. Kobayashi, K. Nonaka, and Y. Shikano, "Stereographical visualization of a polarization state using weak measurements with an optical-vortex beam," *Phys. Rev. A*, vol. 89, 2014, Art. no. 053816.

[34] J. Qiu, C. Ren, and Z. Zhang, "Precisely measuring the orbital angular momentum of beams via weak measurement," *Phys. Rev. A*, vol. 93, 2016, Art. no. 063841.

[35] J. Z. Salvail, M. Agnew, A. S. Johnson, E. Bolduc, J. Leach, and R. W. Boyd, "Full characterization of polarization states of light via direct measurement," *Nature Photon.*, vol. 7, pp. 316–321, 2013.

[36] A. Hariri, D. Curic, L. Giner, and J. S. Lundeen, "Experimental simultaneous readout of the real and imaginary parts of the weak value," *Phys. Rev. A.*, vol. 100, 2019, Art. no. 032119.

[37] L. Luo et al., "Simultaneously precise estimations of phase and amplitude variations based on weak-value amplification," *Appl. Phys. Lett.*, vol. 114, 2019, Art. no. 111104.

[38] X. Zhu, Y. Zhang, S. Pang, C. Qiao, Q. Liu, and S. Wu, "Quantum measurements with preselection and postselection," *Phys. Rev. A*, vol. 84, 2011, Art. no. 052111.

[39] F. Li, J. Huang, and G. Zeng, "Adaptive weak-value amplification with adjustable postselection," *Phys. Rev. A*, vol. 96, 2017, Art. no. 032112.

[40] Z. Li et al., "Retaining high precision and sensitivity for an extended range of phase estimation via modulated weak measurement," *Appl. Phys. Lett.*, vol. 113, 2018, Art. no. 191103.